Emulation of Mycelium's Electrical Activity with Reconfigurable Memristive Spiking Grid

Ioannis K. Chatzipaschalis*†, Ioannis Tompris*, Georgios Kleitsiotis*, Theodoros Panagiotis Chatzinikolaou*, Iosif-Angelos Fyrigos*, Michail-Antisthenis Tsompanas‡, Andrew Adamatzky‡, Phil Ayres§, Antonio Rubio†, and Georgios Ch. Sirakoulis*

* Department of Electrical and Computer Engineering, Democritus University of Thrace, Xanthi, Greece

† Department of Electronic Engineering, Universitat Politècnica de Catalunya, Barcelona, Spain

‡ Department of Computer Science and Creative Technologies, University of the West of England, Bristol, UK

§ Institute of Architecture and Technology, Royal Danish Academy, Copenhagen, Denmark

***Abstract*—Mycelium, the vegetative structure of fungi, exhibits complex electrical signaling patterns when stimulated that resemble neural-like activity, which can be leveraged for bio-inspired computing and sensing applications. To replicate this activity, a 100x100 grid-based circuit has been designed capable of spiking behavior and adaptable configuration thanks to memristive technology aligned with fabricated devices, mimicking the dynamics seen in mycelial networks. Simulations have been carried out to demonstrate that the memristive grid successfully replicates key aspects of mycelium electrical activity recorded from experimental setups, including response to environmental stimuli, spiking signal propagation and eradication.**

***Index Terms*—Memristor, Oscillator, Reconfigurable Hardware, Electrical Activity, Mycelium**

I. Introduction

Engineered living materials (ELMs) are an interdisciplinary field that merges materials science, synthetic biology, and bioengineering to create materials with biological functions and environmental response capabilities [1]. They appear properties such as self-healing, regeneration, and adaptation [2], allowing them to be utilized in sustainable green energy production [3] or biomedical applications [4].

One of the most popular candidates for use in ELMs the last years among the research community is fungi, considered as the largest, widely distributed and oldest group of living organisms [5]. It incorporates the ability to grow and adapt thanks to various environmental but also inherent characteristics that have been studied and modeled [6]–[9]. Its electrical activity, discovered in 1976 [10], is of great interest due to its potential for creating bio-hybrid systems, or digital-twins, for sustainable computing [11], [12].

Memristor is a very promising option for emulating the electrical activity of mycelial cells in novel hardware. First theorized by L. Chua in 1971 [13], memristors are two-terminal electrical analog components that were partially realized at HP Labs in 2008 [14]. Their main advantage is that they can switch between states by changing their conductance in response to applied voltage and then maintaining their state. Their non-volatility and easy incorporation into spiking circuits are therefore essential components for simulating Mycelium's electrical activity with a small, low-power component. There are many fields that they have been utilized. Some of them include security with physical unclonable functions (PUFs) and true random number generators (TRNGs) [15]–[17], solve of optimization problems [18], emulation of brain properties and diseases [19]–[21], and spiking neural networks (SNNs) [22]–[24], demonstrating that they are versatile components, well-suited for a wide range of applications and capable of surpassing traditional hardware performance.

This work introduces a reconfigurable spiking circuit grid using memristors for emulating mycelial electrical activity, including spiking signal propagation [25]–[27], response to environmental stimuli and signal eradication [28], [29]. The spiking properties of RC circuits are being harnessed, as their use is proven in designing mycelial networks with hardware [12]. In Section II the paper provides theoretical background for understanding signal propagation in Mycelium structures, in Section III analyzes proposed circuit for cell and grid architecture, and in Section IV validates the design using fabricated conductive bridge random access memory (CBRAM) devices. In the end, conclusions and future work are presented.

II. Mycelium's Electrical Activity

Studying the electrical activity of real Mycelium structures with experimental set-ups is a really challenging task. However, it is mandatory in order to explore the effects of external stimuli, that is a key factor for further investigation of this material to novel bio-inspired computing applications.

To start off, mycelium appears an electrical activity inherently, which is consistent. However, the amplitude of this signal is very negligible and in the language of circuits can be translated as noise. For that reason, it can not be considered as a signal that propagates and consequently utilized in computing purposes. The interest comes when Mycelium is stimulated externally. In this case, the output signals are spike-like that match the dynamics of a spiking neuron met in brain [25] and can propagate through the hyphae of the material. More specifically, the produced action-potentials rely on the electrically charged Mycelium tips [30]. Also, one can draw analogies of Mycelium's electrical activity with oscillations of electrical potential met in slime mould Physarum polycephalum, where

This work has been supported in part by the FUNGATERIA project, which has received funding from the European Union's HORIZON-EIC-2021-PATHFINDER CHALLENGES program under grant agreement No. 101071145, and by FI SDUR grant, co-financed by AGAUR and the European Union through the European Social Fund Plus (ESF+).

intercellular calcium waves are generated leading to the spike propagation [31].

A. Response to External Factors

The electrical activity of the Mycelium can be affected by multiple external environment factors such as the substrate, the temperature, the pressure, or the existence of various chemical substances [27].

To start with, the substrate's composition play an important role in the output electrical behavior of Mycelium. For instance, moisture content can be changed due time resulting in decreased number of spikes and voltage amplitude as well [28]. Apart from that, it has been experimentally observed that decrease in the electrical activity is met with the application of ethanol (CH_3CH_2OH), while an increase has been noticed when using open flame, mechanical stimulation, or water (H_2O) application. Also, the placement of salt ($NaCl$) through saline solution seems to infer a decrease in the potential of the fruit, but after some time it exhibits trains of spiking activity. This contrary behavior is probably caused due to an osmotic function of the mycelium, resulting from the absorption of saline solution that is then transferred into the fruit caps [29]. Finally, three different experimentally recorded spikes from stimulation with ((D1) saline, (D2) water, and (D3) open flame) are compared with the output of the proposed circuit in Fig. 2(D). The latter appears to have a uniform shape that matches the form of the experimental signals.

III. The Mycelium-inspired Circuit

The simulation and analysis of Mycelium's electrical activity need a circuit composed of several similar components, each representing a tiny segment of the material, capable of transmitting electrical impulses as experimentally seen and discussed in the previous Section II.

A. The Cell's Circuit

To define the basic element of a 2D Mycelium structure, the circuit in Fig. 1 has been conceived. This circuit/cell representing a Mycelium area is able to transmit an electrical signal like the real material. It can be in two different states that are determined by the memristance of the M_{CELL} and represent the existence or the absence of the material, so allowing the transmission or not of the electrical signal. As one can notice, it has multiple inputs and one output that their functionality will be explained at the following lines. Not to mention, that it consists of many different sub-circuits, each of them handles a different operation.

First and foremost, the acquisition sub-circuit consists of four identical resistors $R_{MLN1} = 500\Omega$, that form the Millman's theorem and an AND gate acting as a comparator. Resistances receive the spiking signals from the cell's cardinal neighbors according to Figs. 2(A), and 3 calculate the mean voltage V_{IN_MLN} that is given by Eq. 1 and it is depicted in Fig. 2(C).

$$V_{IN\_MLN} = \frac{\sum \frac{IN_C}{R_{MLN1}}}{\sum \frac{1}{R_{MLN1}}} \tag{1}$$

TABLE I
Truth Table Of A JK Flip-Flop.

J	K	Q_{n+1}
0	0	Q_n
0	1	0
1	0	1
1	1	Q'_n

where IN_C are the voltages of the neighbors with $C \in [N, S, W, E]$. The output V_{IN_D} of this sub-circuit is a pulse with 1V amplitude and width proportional to the time that the neighbors are active, due to the following AND gate that aims to digitize the signal for the appropriate further processing.

After that, an edge detection and activation sub-circuit is used in order to preserve only the first rise of the input signal and for a specific time period. This sub-circuit appears to have a dual role. It protects the unwanted change of the memristance of the M_{CELL} element, and therefore the state of the cell, and also prevents the oscillator of the final stage to be over-excited, allowing the eradication of multiple inputs in one target cell as [29] describes. To achieve this, the digital pulse V_{IN_D} is delayed two times with two different RC circuits. The first one with $R_{D1} = 1k\Omega$ and $C_{D1} = $ 1nF delays the pulse for a little time. This is done to generate an activation signal right after the XOR gate, as it compares the V_{IN_D} with its delayed version and produces the logic '1' during the delay time. This is mandatory for enabling the JK Flip-Flop (JK FF) at a positive generated CLK edge, in order to latch the input pulse V_{IN_D} through its pin J. The second delay circuit with $R_{D2} = 1k\Omega$ and $C_{D2} = 2\mu$F delays the input to ensure that the JK FF will change its state on time regardless the duration of the V_{IN_D}. So, the pin CLK of the JK FF is being driven by V_{CLK} occurring by a second Millman with $R_{MLN2} = 800\Omega$, that combines the two previously referred roles and it is seen in Fig. 2(B). It is also noted that the K pin is constantly supplied with $V_{REF1} = $ 1V, so as to allow the state change of the FF according to Tab. I.

At the next stage of external interference, the output signal from the JK FF V_{FF} will pass through a Single Pole Double Through (SPDT) switch that includes a NMOS and a PMOS transistor and controls whether the cell is at the writing or the propagation mode. At the first one, the cell is being written through T_1 with the help of the IN_{W-EN}, IN_W, and $CTRL$ signals to '0' if it represents an area with no mycelium and to '1' if there is material according to a software generated evolution map as referred in Section IV. At the second one, SPDT passes the JK FF output into its own output to allow the signal propagation if the M_{CELL} is at the LRS. The T_2 ensures that the bottom electrode of the M_{CELL} will be grounded during the writing phase determined by the $CTRL$ signal, in order to be successfully written to the desired memristance value. Also, the diode D along with the $R_{EXT} = 2$kΩ drive the IN_{EXT} signal which is useful for the external stimuli, as well as for the synthesized output from environment sensors related to temperature, humidity etc., that can affect the electrical activity as reported in Section II. In a further expanded work this signal is going to be replaced by a

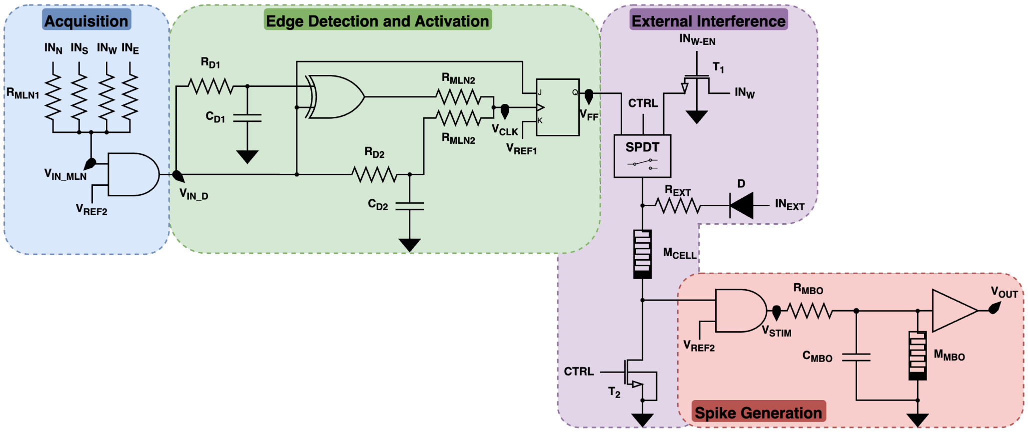

Fig. 1. The proposed circuit for the cell with discrete processing stages.

spike generated by a voltage-controlled oscillator (VCO) [32], that can modulate the output of the environment sensors. So, the external stimuli signal's form will be compatible with the spiking signals produced by the proposed circuit of Fig. 1.

The last sub-circuit is responsible for the spike generation, as the morphology of the electrical signals propagated in mycelium structures shall match with the form of action potentials [29]. Receiving the stimuli voltage $V_{STIM} = 1$V generated by its AND gate with $V_{REF2} = 0.2$V, the Memristive-based Oscillator (MBO) produces an output spiking voltage V_{OUT}, which is then properly amplified with gain $A_V = 5$ and is considered as the cell's output. The MBO consists of an unipolar memristor M_{MBO} in parallel with a capacitor $C_{MBO} = 2$nF and in series with a resistor $R_{MBO} = 2.5\text{M}\Omega$. While the capacitor charges the SET threshold of the memristor is reached. Then, it heads to the LRS state allowing the capacitor to be discharged. When the voltage is low enough, the RESET threshold is met and the memristor closes again to its HRS state allowing the generation of a spike as it is seen in Fig. 2(D).

Finally, regarding the components that have been utilized it is noted that the memristors are based in a compact physics-based model [33], which takes into account the impacts of drift, diffusion, and thermo-diffusion principles and replicates the behavior of CBRAM devices. The formation and breaking of the conductive bridge (CB) between the active and inert electrodes is primarily dependent on temperature and voltage. It also describes both the utilized bipolar and unipolar memristors and has been properly selected for modeling aspects. This particular model has been fitted to compatible fabricated single-layer metal-insulator-metal (MIM) CBRAM devices consisting of Ag ($\sim$ 40nm) / SiO_2 ($\sim$ 20nm) / Pt nanoparticles (NPs) ($\sim$ 5nm) [34], that exhibit quick switching behavior with low voltage thresholds along with low currents in both states for minimizing the power consumption. The digital components have been simulated to have some small delay times that are seen in Tab. II. Also, the utilized transistors have gate length $L = 180$nm, width $W = 9\mu$m, and are bulk CMOS devices based on the Predictive Technology Model (PTM).

TABLE II
DELAYS OF THE UTILIZED DIGITAL COMPONENTS.

Digital Component	Delay (ps)
AND Gate	15
XOR Gate	50
JK Flip-Flop	150

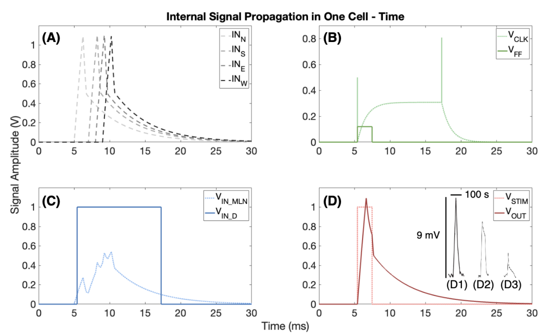

Fig. 2. Internal propagation of the signal in the proposed circuit of Fig. 1. Sub-figures D(1-3) represent recorded spikes from real Mycelium. (D1) from saline after the decrease of the potential, (D2) from water application, and (D3) from thermal stimulation. They have been replicated and properly scaled in accordance with [27], [29].

B. Grid Topology

In order to build a large-scale circuit capable of mimicking the electrical activity of Mycelium, a reconfigurable grid of the previously referred cells has been constructed in a crossbar-like manner. To be more precise, the way of connectivity has been derived from the CA theory. In CAs each cell has a neighborhood that defines its connections with its nearby cells, so that it determines its interaction capabilities.

For this work the von Neumann neighborhood has been

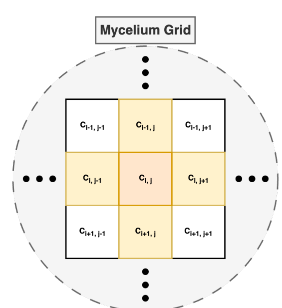

Fig. 3. The grid topology based on the von Neumann neighborhood.

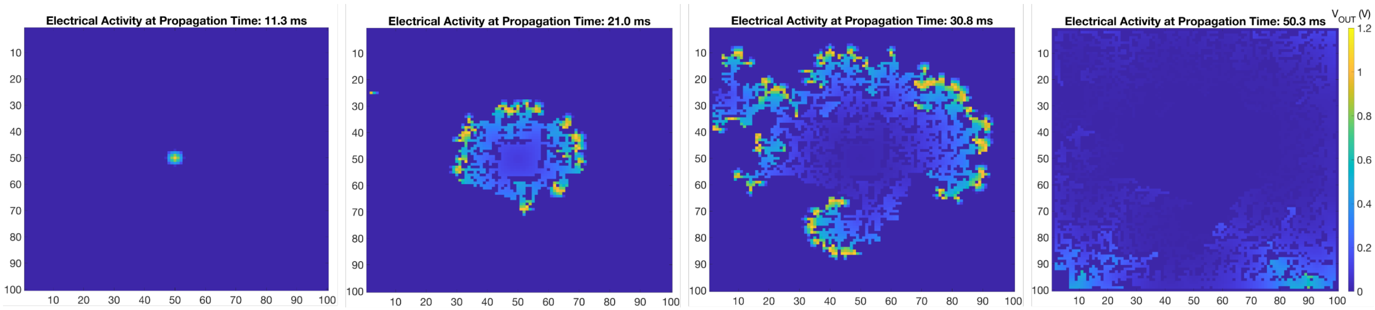

Fig. 4. Propagation of two different external stimuli on the 100×100 grid in different times. The first is at the central cell with coordinates (50, 50), and the second at the cell with coordinates (2, 25).

selected. This neighborhood includes the cell itself and its four orthogonal neighbors (north, south, west, east) as one can notice in Fig. 3. In this way, it covers a diamond shape around the central cell with a radius of 1 (five cells in total). The reasons that make it more appropriate for the emulation of the fungal electrical activity, especially in hardware, are the low computational cost, and the forming of targeted pathways. Due to the first reason, large-scale simulations can be faster without sacrificing too much accuracy. Regarding the second one, it is noted that the electrical signals only travel along the cardinal directions. So, they follow a clear, directional, and more efficient path along a specific hyphal strand or branch of the Mycelium, thus creating a more focused, channel-like propagation.

Using this topology, a reconfigurable 100×100 grid has been designed as Fig. 3 showcases. The modeling scale involves discretizing space into square lattice sites, each with a side length of 100μm [8], encompassing a simulated grid area of 1cm^2. It is also noted, that the boundary conditions of the grid are null to better mimic a real Mycelium structure by signifying the and of the material.

IV. Simulation Results

For the validation of the designed circuit, simulations in various test cases have been carried out with the Cadence Virtuoso Design Suite. In order to create a realistic mycelial map, a reaction-diffusion model has been used [7]. The produced map is a 2D 100x100 table indicating the presence or absence of Mycelial material on the grid. Then, this table has been used to properly write the crossbar-like grid in order to represent a circuitry structure of the ELM on top of that the electrical activity is being studied.

As one can notice from Fig. 4, a test case with two different external stimulations has been performed. The external stimulation is a pulse that excites the cell from its IN_{EXT} pin. It has amplitude equal to 0.4V and duration of 1ms. The first one happens at $t = 10$ms in the center of the grid forcing the enabled neighbors to contribute to the signal propagation. After another 10ms from the initial stimulation, a second cell with coordinates (2, 25) is triggered. It is observed that the time that the two signals meet each other they both trigger the cells of the meeting points and then depreciate. This phenomenon of mutual signal eradication is

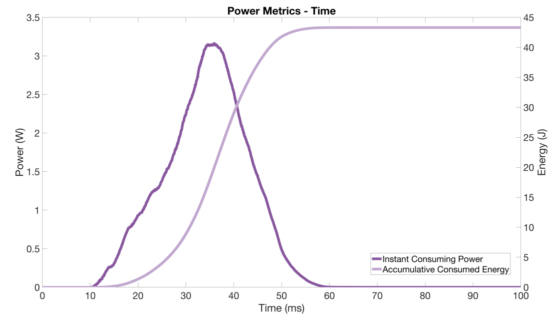

Fig. 5. Power metrics of the grid across propagation time.

also met in modeling with fungal automaton implemented in software [29]. After some time with no extra simulations the propagation is being completed and the grid returns to its equilibrium state with no output voltage noticed from any cell.

Other than that, some power metrics have been also exported. In Fig. 5 dark purple curve represents the instant consuming power of the whole grid with a peak of 3.16W the time that most of cells propagate a signal. After propagation time $t = 60$ms the last cells go inactive and the power is minimized considerably, while after some time returns to its lowest idle value near zero. Finally, the light purple curve depicts the accumulated consumed energy with a total value, after the propagation of the two stimuli, equal to 43.3J.

V. Conclusions and Future Work

This work demonstrates the emulation of mycelium-like electrical activity using a reconfigurable memristive grid. Propagation characteristics such as response to environmental stimuli, spiking signal propagation and eradication observed in real mycelial structures have been replicated.

Future work includes the integration of environmental sensors that will provide spiking-compatible stimuli, paving the way for use of this framework in real-time applications. Also, an evolution map of real mycelium structures is going to be harnessed instead of the modeled one, to study the electrical activity in an even more realistic manner. Thus, a digital-twin represented by the proposed grid can be exploited, and with the help of an interface will be in position to interact with a real Mycelium-based ELM.

References

[1] C. Gilbert and T. Ellis, "Biological engineered living materials: growing functional materials with genetically programmable properties," *ACS synthetic biology*, vol. 8, no. 1, pp. 1–15, 2018.

[2] A. Mora-Boza, S. Acosta, and M. Puertas-Bartolomé, "Biopolymers for the development of living materials for biomedical applications," in *Biopolymers*. Elsevier, 2023, pp. 263–294.

[3] B. An, Y. Wang, Y. Huang, X. Wang, Y. Liu, D. Xun, G. M. Church, Z. Dai, X. Yi, T.-C. Tang *et al.*, "Engineered living materials for sustainability," *Chemical Reviews*, vol. 123, no. 5, pp. 2349–2419, 2022.

[4] A. Rodrigo-Navarro, S. Sankaran, M. J. Dalby, A. del Campo, and M. Salmeron-Sanchez, "Engineered living biomaterials," *Nature Reviews Materials*, vol. 6, no. 12, pp. 1175–1190, 2021.

[5] M. J. Carlile, S. C. Watkinson, and G. W. Gooday, *The fungi*. Gulf Professional Publishing, 2001.

[6] V. Carlström, A. Rigobello, and P. Ayres, "Modelling of morphogenesis to support the design of fungal-based engineered living materials," *Research Directions: Biotechnology Design*, vol. 2, p. e11, 2024.

[7] I. Tompris, I. K. Chatzipaschalis, T. P. Chatzinikolaou, I.-A. Fyrigos, M.-A. Tsompanas, A. Adamatzky, P. Ayres, and G. C. Sirakoulis, "A reaction-diffusion cellular automata model for mycelium-based engineered living materials evolution," in *International Conference on Cellular Automata for Research and Industry*. Springer, 2024, pp. 253–264.

[8] M. D. Fricker, L. L. Heaton, N. S. Jones, and L. Boddy, "The mycelium as a network," *The fungal kingdom*, pp. 335–367, 2017.

[9] I. K. Chatzipaschalis, I. Tompris, K. Rallis, T. P. Chatzinikolaou, I.-A. Fyrigos, M.-A. Tsompanas, A. Adamatzky, P. Ayres, A. Rubio, and G. C. Sirakoulis, "Mycelium-based elm digital twin implemented in fpga," in *International Conference on Cellular Automata for Research and Industry*. Springer, 2024, pp. 265–276.

[10] C. L. Slayman, W. S. Long, and D. Gradmann, ""action potentials" in neurospora crassa, a mycelial fungus," *Biochimica et Biophysica Acta (BBA)-Biomembranes*, vol. 426, no. 4, pp. 732–744, 1976.

[11] N. Roberts and A. Adamatzky, "Mining logical circuits in fungi," in *Fungal machines: sensing and computing with fungi*. Springer, 2023, pp. 311–321.

[12] A. Adamatzky, P. Ayres, A. E. Beasley, N. Roberts, and H. A. Wösten, "Logics in fungal mycelium networks," *Logica Universalis*, vol. 16, no. 4, pp. 655–669, 2022.

[13] L. Chua, "Memristor-the missing circuit element," *IEEE Transactions on Circuit Theory*, vol. 18, no. 5, pp. 507–519, 1971.

[14] D. B. Strukov, G. S. Snider, D. R. Stewart, and R. S. Williams, "The missing memristor found," *nature*, vol. 453, no. 7191, pp. 80–83, 2008.

[15] S. Singh, F. Zahoor, G. Rajendran, V. Rana, S. Patkar, A. Chattopadhyay, and F. Merchant, "Integrated architecture for neural networks and security primitives using rram crossbar," in *2023 21st IEEE Interregional NEWCAS Conference (NEWCAS)*. IEEE, 2023, pp. 1–5.

[16] A. Malik and C. Papavassiliou, "A memristive true random number generator," in *2023 30th IEEE International Conference on Electronics, Circuits and Systems (ICECS)*. IEEE, 2023, pp. 1–4.

[17] D. Arumi, S. Manich, A. Gómez-Pau, R. Rodríguez-Montañés, M. González, and F. Campabadal, "True random number generator based on rram-bias current starved ring oscillator," *IEEE Journal on Exploratory Solid-State Computational Devices and Circuits*, 2023.

[18] M. Graber and K. Hofmann, "An integrated coupled oscillator network to solve optimization problems," *Communications Engineering*, vol. 3, no. 1, p. 116, 2024.

[19] E. Salvador, R. Rodriguez, E. Miranda, J. Martin-Martinez, A. Rubio, A. Crespo-Yepes, V. Ntinas, G. C. Sirakoulis, and M. Nafria, "Noise-induced homeostasis in memristor-based neuromorphic systems," *IEEE Electron Device Letters*, 2024.

[20] I. K. Chatzipaschalis, I. Tompris, E. Stavroulakis, T. P. Chatzinikolaou, I.-A. Fyrigos, P. Fraidakis, A. Calomarde, R. Gomá, G. C. Sirakoulis, and A. Rubio, "A spatio-temporal-based concept for associative memory modeling with memristors," in *2024 IEEE 24th International Conference on Nanotechnology (NANO)*. IEEE, 2024, pp. 545–550.

[21] I. K. Chatzipaschalis, E. Tsipas, I.-A. Fyrigos, A. Rubio, and G. C. Sirakoulis, "Cbram-based bio-inspired circuit for the emulation and treatment of the parkinson's disease," *IEEE Transactions on Circuits and Systems II: Express Briefs*, 2023.

[22] J. H. Quintino Palhares, N. Garg, P.-A. Mouny, Y. Beilliard, J. Sandrini, F. Arnaud, L. Anghel, F. Alibart, D. Drouin, and P. Galy, "28 nm fdsoi embedded pcm exhibiting near zero drift at 12 k for cryogenic snns," *npj Unconventional Computing*, vol. 1, no. 1, p. 8, 2024.

[23] T. Stecconi, V. Bragaglia, M. J. Rasch, F. Carta, F. Horst, D. F. Falcone, S. C. Ten Kate, N. Gong, T. Ando, A. Olziersky *et al.*, "Analog resistive switching devices for training deep neural networks with the novel tiki-taka algorithm," *Nano Letters*, vol. 24, no. 3, pp. 866–872, 2024.

[24] T. P. Chatzinikolaou, I. K. Chatzipaschalis, K.-A. Tsakalos, R.-E. Karamani, I.-A. Fyrigos, S. Kitsios, P. Bousoulas, D. Tsoukalas, and G. C. Sirakoulis, "Recognition of greek alphabet characters with memristive neuromorphic circuit," in *2023 IEEE International Conference on Metrology for eXtended Reality, Artificial Intelligence and Neural Engineering (MetroXRAINE)*. IEEE, 2023, pp. 1209–1214.

[25] R. Mayne, N. Roberts, N. Phillips, R. Weerasekera, and A. Adamatzky, "Propagation of electrical signals by fungi," *Biosystems*, vol. 229, p. 104933, 2023.

[26] A. Adamatzky, "Language of fungi derived from their electrical spiking activity," *Royal Society Open Science*, vol. 9, no. 4, p. 211926, 2022.

[27] ——, "Action potential like spikes in oyster fungi pleurotus djamor," in *Fungal Machines: Sensing and Computing with Fungi*. Springer, 2023, pp. 3–13.

[28] N. Phillips, A. Gandia, and A. Adamatzky, "Electrical response of fungi to changing moisture content," *Fungal Biology and Biotechnology*, vol. 10, no. 1, p. 8, 2023.

[29] A. Adamatzky, "Towards fungal computer," *Interface focus*, vol. 8, no. 6, p. 20180029, 2018.

[30] P. Hunter, "The fungal grid," *EMBO reports*, 2023.

[31] A. Adamatzky, M. Tegelaar, H. A. Wosten, A. L. Powell, A. E. Beasley, and R. Mayne, "On boolean gates in fungal colony," *Biosystems*, vol. 193, p. 104138, 2020.

[32] I. K. Chatzipaschalis, T. P. Chatzinikolaou, I.-A. Fyrigos, A. Rubio, and G. C. Sirakoulis, "A memristive neuromorphic voltage-to-frequency mapping oscillator for automotive applications," in *2023 18th International Workshop on Cellular Nanoscale Networks and their Applications (CNNA)*. IEEE, 2023, pp. 1–4.

[33] I.-A. Fyrigos, T. P. Chatzinikolaou, V. Ntinas, S. Kitsios, P. Bousoulas, M.-A. Tsompanas, D. Tsoukalas, A. Adamatzky, A. Rubio, and G. C. Sirakoulis, "Compact thermo-diffusion based physical memristor model," in *2022 IEEE International Symposium on Circuits and Systems (ISCAS)*. IEEE, 2022, pp. 2237–2241.

[34] P. Bousoulas, D. Sakellaropoulos, C. Papakonstantinopoulos, S. Kitsios, C. Arvanitis, E. Bagakis, and D. Tsoukalas, "Investigating the origins of ultra-short relaxation times of silver filaments in forming-free SiO_2-based conductive bridge memristors," *Nanotechnology*, vol. 31, no. 45, p. 454002, 2020.